GA–A27413

TURBULENCE AND TRANSPORT RESPONSE TO RESONANT MAGNETIC PERTURBATIONS IN ELM-SUPPRESSED PLASMAS ON DIII-D

by
G.R. McKEE, Z. YAN, C. HOLLAND, R.J. BUTTERY, T.E. EVANS,
R.A. MOYER, S. MORDIJCK, R. NAZIKIAN, T.L. RHODES,
O. SCHMITZ and M.R. WADE

OCTOBER 2012

GENERAL ATOMICS

DISCLAIMER

GA–A27413

TURBULENCE AND TRANSPORT RESPONSE TO RESONANT MAGNETIC PERTURBATIONS IN ELM-SUPPRESSED PLASMAS ON DIII-D

by
G.R. McKEE,[1] Z. YAN,[1] C. HOLLAND,[2] R.J. BUTTERY, T.E. EVANS,
R.A. MOYER,[2] S. MORDIJCK,[3] R. NAZIKIAN,[4] T.L. RHODES,[5]
O. SCHMITZ[6] and M.R. WADE

This is a preprint of a paper to be presented at the 24th IAEA Fusion Energy Conference, October 8–13, 2012 in San Diego, California and to be published in the Proceedings.

[1]University of Wisconsin-Madison, Madison, Wisconsin USA
[2]University of California San Diego, La Jolla, California USA
[3]College of William and Mary, Williamsburg, Virginia USA
[4]Princeton Plasma Physics Laboratory, Princeton, New Jersey USA
[5]University of California Los Angeles, Los Angeles, California USA
[6]Forschungszentrum, Jülich, GmbH, Jülich, Germany

Work supported by the
U.S. Department of Energy under
DE-FG02-89ER53296, DE-FG02-08ER54999,
DE-FC02-04ER54698, DE-FG02-07ER54917,
DE-FG02-05ER54809, DE-AC02-09CH11466
and DE-FG02-08ER54984

GENERAL ATOMICS PROJECT 30200
OCTOBER 2012

ABSTRACT

Long wavelength turbulence increases dramatically in the outer regions of DIII-D plasmas with the application of radial resonant magnetic field perturbations (RMP) to suppress edge-localized modes (ELMs). Correspondingly, transport increases and global energy confinement decreases in these low collisionality RMP-ELM suppressed discharges. This process is evident through a sharp reduction in core and pedestal density, while ion and electron temperatures may change only slightly. Low wavenumber density turbulence ($k_\perp \rho_i < 1$) in the range of 60–300 kHz, measured with beam emission spectroscopy (BES), is modified and generally increases throughout the outer region ($0.6 < \rho < 1.0$) of the plasma in response to RMPs over a range of q_{95} values; ELM suppression, in contrast, occurs for a narrower range in q_{95}. Radial magnetic field modulation experiments indicate that these turbulence modifications occur on a time scale of a few milliseconds or less near $\rho = 0.85–0.95$, significantly faster than transport time-scales and faster than the local pressure gradients and shearing rates evolve at these locations. As the internal coil current is varied from 3.2 to 4.2 kA, the turbulence magnitude varies in phase by 30% or more, while local density changes by only a few percent. This dynamical behavior suggests that the turbulence is directly affected by the RMP, which may partially or largely explain the resulting increased transport and stabilization of the pedestal against peeling-ballooning instabilities that are thought to drive ELMs. Understanding this transport process will be crucial to extrapolating and optimizing the RMP ELM-suppression technique in ITER.

1. INTRODUCTION

The application of resonant magnetic perturbations (RMP) to H-mode plasmas successfully suppressed Edge Localized Modes (ELMs) on DIII-D [1]. RMP ELM suppression is typically accompanied by a modest to significant reduction of particle and energy confinement. Mitigating or suppressing ELMs is of critical importance to ITER and future burning plasmas due to the damaging effects of highly localized, periodic intense bursts of particles and energy associated with ELMs. ELMs cause the rapid expulsion of heat and particles, with transient high heat fluxes on divertor surfaces. In modern experiments with graphite and metal walls, the energy and particle bursts associated with ELMs are generally not problematic, however extrapolation to reactor conditions with the reduced surface area-to-volume ratios of burning plasma experiments will result in predicted ELM energy fluxes of up to 20 MJ in fractions of a millisecond. Such large bursts will erode plasma-facing components, generate impurities, and shorten divertor lifetimes, and so it is essential to mitigate or suppress these deleterious ELMs while retaining the good confinement and stability properties of H-mode tokamak plasmas to advance the development of fusion energy systems. Extrapolating the RMP ELM-suppression technique to ITER and fusion reactors thus requires a comprehensive understanding of the physical mechanisms by which RMPs mitigate ELMs, as well as the implications for transport and confinement.

Long wavelength density fluctuations increase rapidly and significantly in the outer regions of DIII-D plasmas with the application of these RMPs to suppress ELMs [2]. Correspondingly, particle transport is increased and global energy confinement decreased in these low collisionality RMP-ELM suppressed discharges [3]. This process is evident through a reduction in core and pedestal density, which has been quantified through perturbative gas-puff-modulation studies, as well as interpretative modeling of density sources and sinks [4]. Low and intermediate wavenumber turbulence ($k_\perp \rho_i < 2$), measured with beam emission spectroscopy (BES) [5] and Doppler backscattering [6], is modified and generally increases throughout the outer region of the plasma in response to RMPs. The dynamical behavior suggests that the turbulence is directly affected by the RMP, which may partially or largely explain the resulting increased transport and stabilization of the pedestal against peeling-ballooning instabilities that are thought to drive ELMs [7]. Radial magnetic field modulation experiments indicate that the turbulence modifications occur significantly faster than transport time-scales and also faster than local pressure and gradients therein (turbulence drive terms) and flow shear (stabilization) evolve [2]; this suggests a new turbulence drive mechanism associated with the RMP that may be crucial to the resulting enhanced transport. Understanding this process is crucial to extrapolating this ELM-suppression method to ITER.

On DIII-D, radial magnetic fields are applied through a set of 12 internal window-frame coils: 6 coils are above the midplane, and 6 below, allowing for application of static n=3 perturbations. The coil current can be operated statically or dynamically. Most experiments are performed with even parity, in which the upper and lower pairs of coils have the same current

polarity. Experiments have been run with n=2 configuration, which can be toroidally rotated. Currents of up to 6 kA can be applied to these coils, providing a radial field of about 50 Gauss near the plasma surface under vacuum conditions. Currently, it is planned to install a set of internal coils on ITER to perform ELM suppression through a similar method.

The global confinement performance of plasmas is strongly dependent on the height of the pedestal temperature: a strong positive correlation is found between the temperature of the pedestal and the core temperature, and therefore the fusion reactivity and efficiency of the plasma as a fusion energy generation system [8]. This study examines the response of global plasma parameters and profiles to RMPs (Section 2), as well as the changes to turbulence that accompany application of RMP. The results of a radial field modulation experiment that examines the dynamics of turbulence and local parameter changes are presented in Section 3, while Section 4 presents the correlation of turbulence changes associated with q_{95}, which may suggest a link to why RMP ELM suppression occurs most readily for certain ranges and values of q_{95}.

2. PLASMA PROFILE AND TRANSPORT CHANGES WITH RMP

ELMs are suppressed via application of Resonant Magnetic Perturbations under particular plasma conditions. These include relatively low collisionality, and operation within specific ranges of q_{95}; q_{95}~3.5 is typically required to get optimal ELM suppression with the n=3 upper/lower internal coil configuration on DIII-D, though other ranges of q_{95} exist for ELM suppression [9]. ELM suppression has also been obtained in moderately high collisionality and density plasmas [1]. An example of ELM suppression at low collisionality is shown in Fig. 1, exhibiting the evolution of an H-mode discharge, 145384 (B_T = –1.9 T, I_p=1.5 MA, q_{95}=3.5), with RMPs applied to suppress ELMs starting at 2400 ms (indicated by dashed line.) The coil current ramps up to 4.25 kA from 2350–2400 ms and is held constant until 2900 ms, after which is modulated, shown in Fig. 1(c) (the modulation is discussed later.) The edge recycling hydrogenic Balmer-

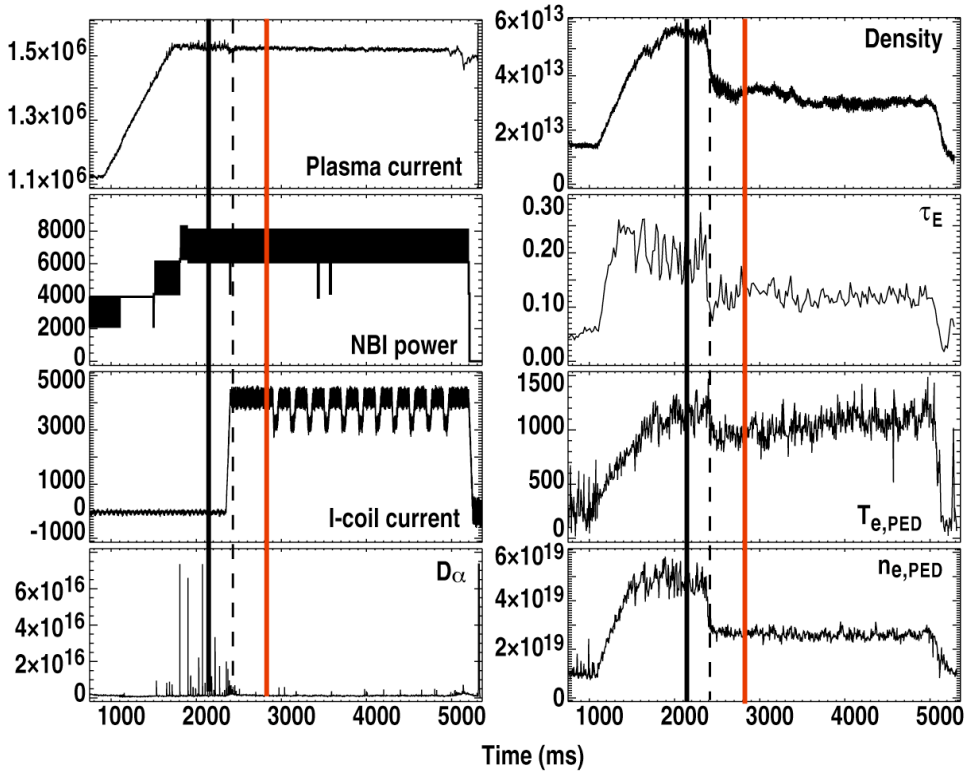

FIG. 1. Discharge evolution for RMP ELM-suppressed discharge: (a) plasma current; (b) injected neutral beam power; (c) internal coil current; (d) recycling D_α emission; (e) line integrated density; (f) energy confinement time; (g) pedestal electron temperature height; (h) pedestal electron density.

alpha emission [Fig. 1(c)] quickly changes, with an initial burst of higher frequency, lower amplitude ELMs that are then completely suppressed. ELMs remain suppressed for the duration of the I-coil current, with the exception of small bursts during the I-coil modulation transitions. Several global and local plasma responses take place with the application of RMPs via the internal coils. The line-integrated density decreases significantly [Fig. 1(e)], while the core

electron temperature is relatively unperturbed. The strong reduction in density, identified as "density pump-out," is a common feature of low-collisionality RMP discharges. In particular, density pump-out is often observed with magnetic perturbations, regardless of whether ELMs are suppressed. Global energy confinement time, τ_E, is reduced from near 0.20 s to about 0.14 s during the RMP phase.

The H-mode pedestal also exhibits a dramatic reduction in the density height [Fig. 1(g)], with only modest changes to the electron temperature height [Fig. 1(h)]. This phenomenology is fairly typical of RMP ELM-suppressed discharges, though the magnitude of the density pump-out and changes in global energy confinement and rotation can be mitigated through optimization of plasma shape, density, input power, and I-coil current.

Profiles for several parameters are compared for standard ELMy H-mode phase (t=2180 ms) and the RMP ELM-suppressed phase (t=2800 ms) in Fig. 2; changes are consistent with the global effects shown previously. The density profile undergoes a broad reduction [Fig. 2(a)] across the full profile, with the pedestal narrowing and the pedestal gradient reducing slightly. Interestingly, the core ion temperature rises moderately for $r/a < 0.4$ [Fig. 2(b)], while electron temperature decreases very slightly across most of the profile [Fig. 2(d)]. The rotation profile [Fig. (2(c)] exhibits a more complex modification, with the profile flattening in the outer half radius, while the core rotation actually increases modestly. Naturally, this alters the ExB shear for the pedestal and core region. The increased central ion temperature and rotation can be explained through reduced density at similar injected beam power (increased energy and angular momentum per ion) along with corresponding transport changes.

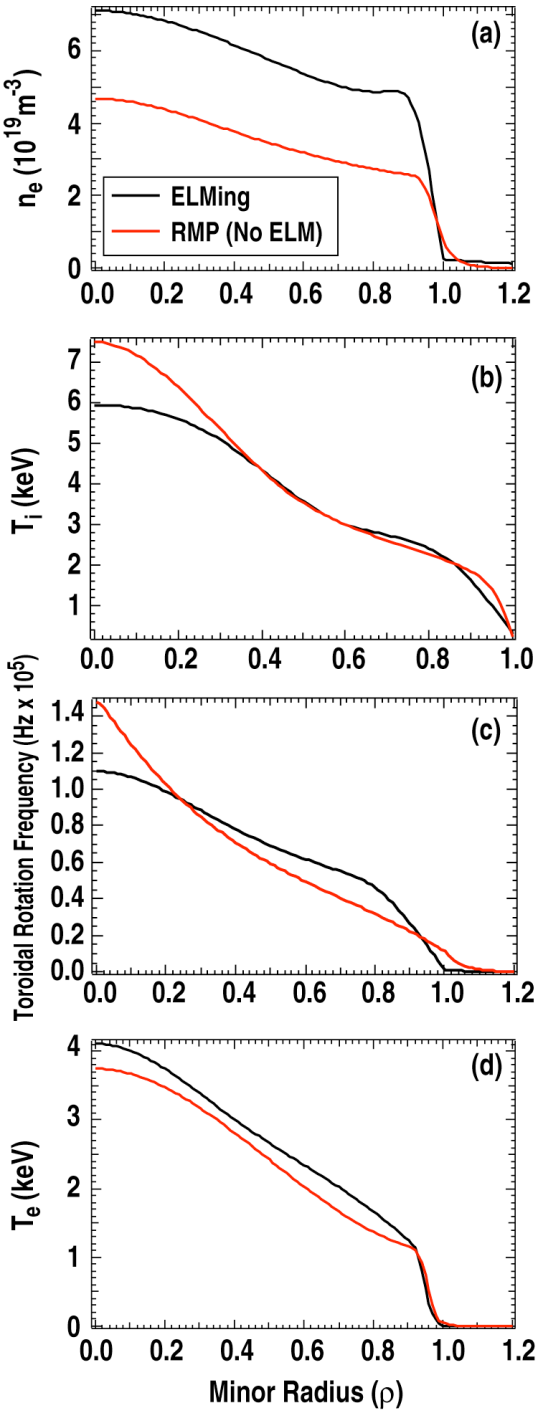

Fig. 2. Profiles of (a) electron density (Thomson scattering); (b) ion temperature (CER); (c) toroidal rotation (CER); (d) electron temperature (Thomson + ECE.)

The inferred ion and electron thermal diffusivities are shown in Fig. 3. Thermal diffusivity is seen

to increase for both ion and electron channels across much of the plasma radius. This is consistent with reduced energy confinement and increased turbulence, discussed next.

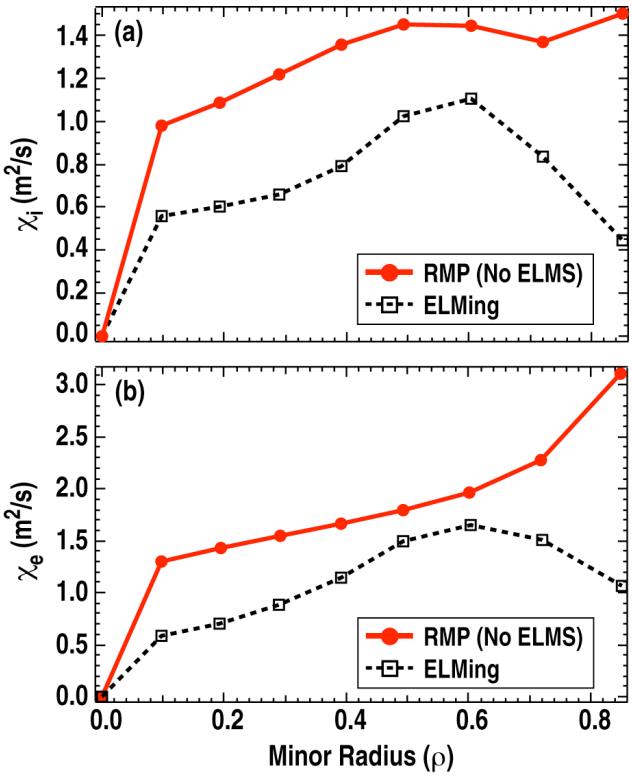

FIG. 3. Comparison of (a) ion thermal diffusivity and (b) electron thermal diffusivity in ELMing and RMP ELM-suppressed phases.

3. TURBULENCE CHARACTERISTICS AND DYNAMIC RESPONSE TO RMP

Long-wavelength $(k_\perp \rho_I < 1)$ density fluctuations are observed to change dramatically in response to applied RMP fields. By examining the turbulence response over a wide radial range from the pedestal to the core, and at several wavenumber ranges, and by looking at the dynamic response of turbulence to modulated radial fields, an emerging picture is developing that suggests direct turbulence modification by the RMP fields plays a crucial role in the transport changes and ultimately in effecting the suppression of ELMs. The process is complex and the plasma response depends on a number of crucial plasma parameters (collisionality, rotation, q_{95}).

The spectra of long-wavelength density fluctuations obtained with Beam Emission Spectroscopy (BES) at $\rho = 0.75$ in ELMing and RMP ELM-suppressed phases of an H-mode plasma are compared in Fig. 4(a), illustrating the dramatic increase in turbulence with application of RMP. The amplitude of broadband density fluctuations in the frequency range 60–350 kHz increases significantly (the fluctuations below 60 kHz are dominated by beam fluctuations that are larger than any local plasma turbulence.) It is observed that the peak of the broadband fluctuation spectrum moves to lower frequency (from approximately 180 kHz in ELMing phase, to near 120 kHz during the RMP phase). This reflects primarily a reduction in the local radial electric field (reduced rotation) and corresponding Doppler shift.

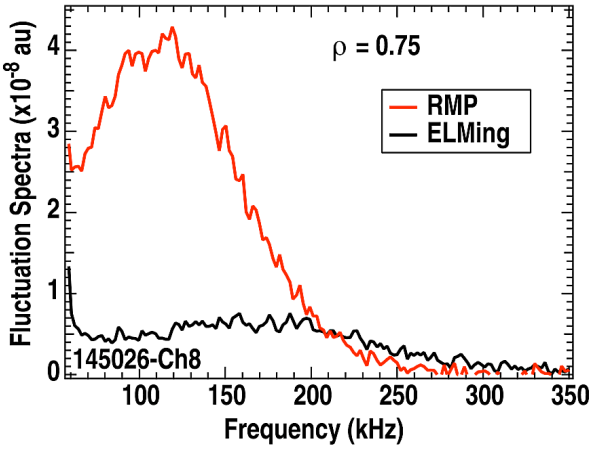

FIG. 4. Comparison of density fluctuation spectra for low-k density fluctuations (BES) at r=0.75 with and without RMP.

It was seen in Section 2 that pressure and rotation (shear) profiles change significantly as a consequence of applied RMP. Since temperature and density gradients provide the dominant free energy source for turbulence, and radially sheared ExB flow provides a stabilizing mechanism [10], it is crucial to determine whether the experimentally observed turbulence changes result from changes in these profile driving and damping terms that are altered with RMP, or result from other mechanisms such as a direct effect of the radial magnetic field on the fully saturated turbulence state. To address this question, a series of rapid modulations in the RMP field were applied to an ELM-suppressed discharge.

The fast dynamical changes in the turbulence, flows, and associated gradients address these questions by allowing for an examination of the spatiotemporal correlations and response of local turbulence, plasma parameters and gradient. Figure 5(a) illustrates the variation of long-wavelength density fluctuations, measured with BES inside the pedestal region (ρ=0.88), to such modulated radial fields [Fig. 5(a)]. Fluctuations can be seen to rise and fall with the internal coil current [Fig. 5(b)] across a broad spectral range: 60–200 kHz. The temporal response is quantified in Fig. 5(c) which integrates the fluctuations spectrally (red curve) and phase locks to multiple modulation cycles (to improve signal to noise for fast measurements). As fluctuations increase, local density decreases. The fluctuation changes are mapped to density changes (also measured locally via BES) in Fig. 5(d), during the radial field modulation cycle. This dependence indicates that turbulence changes lead local density modifications. Note also that the local density change is small (~5%) during the modulation cycle, while the fluctuation magnitude oscillates by ~30%. A similar temporal analysis of the local density gradient and fluctuations shows no clear correlation between the two quantities.

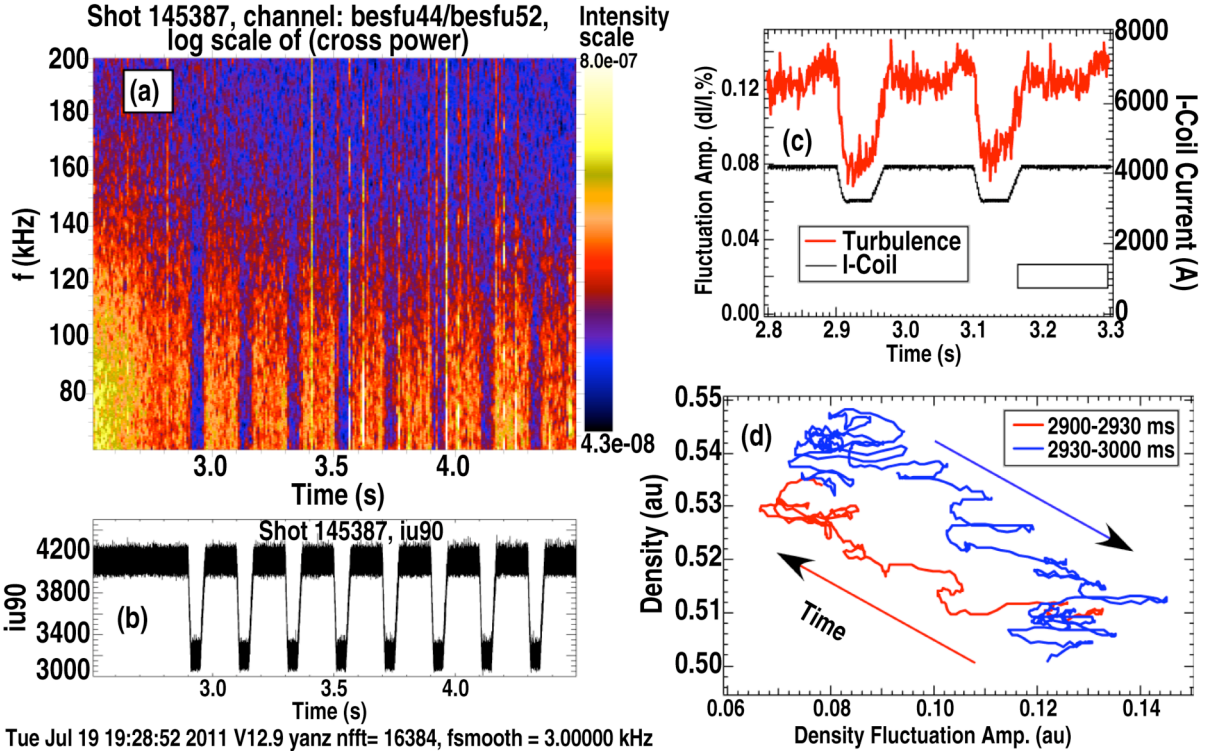

FIG. 5. (a) Spectrogram of density fluctuations from BES during a modulated RMP ELM-suppressed discharge, (b) internal coil current (suppressed zero), (c) integrated low-k fluctuation evolution at ρ=0.88, (d) relation of density fluctautions to local density.

The poloidal velocity of the turbulence is directly measured via time-lag correlation analysis with the 2D BED array [11]. The turbulence poloidal velocity has been shown quantitatively to be very similar to the local ExB velocity [12], as is expected since any diamagnetic velocities are small. The correlation between velocity and coil current is shown in Fig. 6. Figure 6(a) shows the

evolution at higher-time resolution, which is relatively noisy (gray-dashed), as well as smoothed data (red-solid) near r/a=0.86, just inside the pedestal. The velocity clearly increases (decreases) as internal coil decreases (increases). The response time is slower than the density fluctuation amplitude response time near r/a=0.8–0.9. Furthermore, a radial profile of poloidal turbulence velocity [Fig. 6(b)] shows a relatively uniform rise and fall, suggesting little change in the local shearing rates. The slower response of the local poloidal turbulence velocity suggests that fast shear flow modification is not primarily responsible for the rapid turbulence changes with RMP.

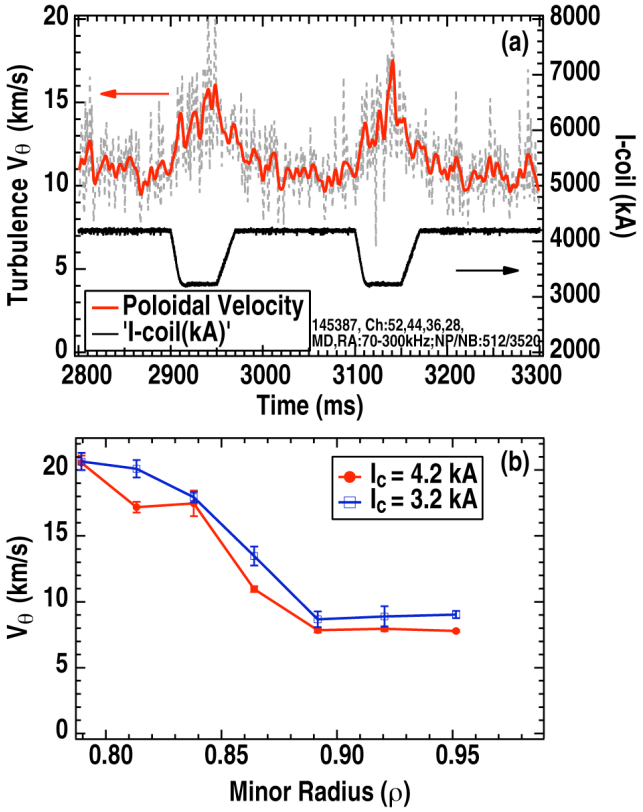

FIG. 6. Poloidal turbulence velocity during field modulations: (a) evolution at high time resolution (gray), and smoothed (red) at r/a=0.86, on left axis, compared with coil current (right axis); (b) time-averaged profile of turbulence velocity at high (4.2 kA) and low (3.2 kA) internal coil current phases.

These measurements thus indicate that the turbulence is responding rapidly (on a scale of a few milliseconds or less) just inside the pedestal region ($0.75 < r/a < 0.95$) to the applied RMP fields, and faster than driving (gradient) or damping (rotation) terms. This suggests that the RMP is directly affecting the turbulence through another mechanism. It has been suggested from a theoretical perspective that damping of zonal flows occurs with radial fields, and may be a mechanism by which turbulence can be directly and rapidly affected by the RMP [13]. The 2D BES density fluctuation can potentially allow for measurements of zonal flow signatures [14,15]; to date, application of Time-Delay-Estimation methods to poloidally resolved BES measurements [16] in these RMP ELM-suppressed discharges has not demonstrated the presence of zonal flow activity with RMP; this study is continuing.

4. TURBULENCE VARIATION DURING *q*-PROFILE SCAN: CONNECTION TO LOW-ORDER RATIONAL SURFACES

RMP ELM suppression depends sensitively on q_{95}, and ELMs are most readily suppressed for particular ranges of q_{95}. It has been shown that this correlates with the overlap between the poloidal mode structure of the radial field perturbation, and the corresponding safety factor profile in the outer radial range of the plasma [17]. To examine this behavior and to search for possible connections to local turbulence amplitude and dynamics, plasma current was varied in a single discharge with an applied radial magnetic field. Figure 7 shows the evolution of plasma current, q_{95} and recycling D_α emission. Bands of ELM suppression are clearly observed for values of q_{95} near 3.9 and 3.45, with weaker suppression windows near 3.35 and 3.55.

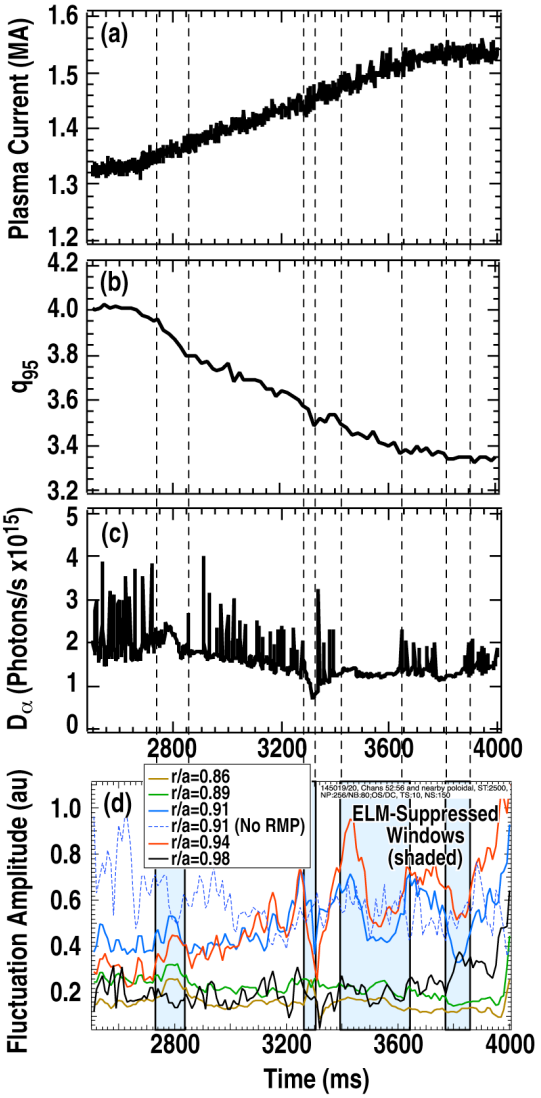

FIG. 7. Evolution of (a) plasma current; (b) q_{95}; (c) recycling D_α light during a q_{95} ramp with applied radial magnetic field perturbations; (d) density fluctuation amplitude measured with BES at several radial locations.

BES measurements of density fluctuations were acquired at the outboard midplane during this scan. Density fluctuations were integrated over a frequency window of ~60–300 kHz with a time window of 20 ms. The fluctuation amplitude evolution during this scan of q_{95} is shown for several radii in Fig. 7(d); ELM-suppression windows are shaded blue. The fluctuation amplitude exhibits significant variation at the start and end of ELM-suppression windows, and a strong radial dependence to the fluctuation dynamics is found. During the first ELM-suppression window (2730–2850 ms), fluctuations are seen to rise and then fall for $0.86 < r/a < 0.94$, while in the pedestal itself (r/a~0.98), fluctuations drop modestly. During the primary ELM suppression window (q_{95}~3.45), a large and rapid rise and subsequent fall in fluctuations is seen for 0.88–0.92, with little change at other locations; pedestal fluctuations (black, r/a~0.98) are seen to increase near 3800 ms (q_{95}~3.35), while a decrease in fluctuations is seen on the top of the pedestal region (0.9–0.93). Finally, a short but sharp rise and fall is seen over this radial zone (0.9–0.93) for the short ELM-suppression window seen at 3250–3300 ms (q_{95}~3.55).

A similar discharge without application of radial magnetic fields is compared at one radial location. Overlaid in Fig. 7(d) (blue dashed trace) are fluctuation amplitude at ρ=0.91 with no radial field. The fluctuations evolve locally much differently and have no connection to the value of q_{95}. As expected, ELMs are continuous throughout this time period in this reference discharge (no RMP). This comparison demonstrates that the turbulence dynamic behavior is particular to the combination of both q_{95} and radial field, and the sharp changes in turbulence occurs explicitly as the discharge evolves from ELMing to ELM-suppressed, and back.

The complex spatial and temporal dynamics of the fluctuation amplitudes are clearly correlated with the ELM-suppression windows, but which changes are related to or driving the others is not yet clear. Further investigation of the fast temporal behavior of turbulence and flows and potential connections to low-order rational q-surfaces will be pursued.

5. SUMMARY AND CONCLUSIONS

Taken together, these measurements indicate that the radial magnetic field appears to directly and rapidly cause the increased turbulence, and is not acting primarily by changing local quantities, their gradients, or shear. The mechanism is unclear, but it has been hypothesized that RMPs may damp zonal flows and thereby cause an increase in turbulence and transport, consistent with these results.

While the overall response of turbulence and transport to RMP is complex owing to the highly nonlinear interactions between the plasma profiles and gradients therein as well as radial magnetic field perturbations, these new measurements of fluctuations suggest that a direct turbulence mechanism mediates the interaction between RMP fields and local transport. This mechanism may play a major role in the ELM suppression process. Elucidating this connection and the possible role of zonal flow behavior will be critical to projecting this ELM suppression technique to ITER and other burning plasma experiments.

REFERENCES

[1] EVANS, T.E., *et al.*, Nucl. Fusion **45** (2005) 595.

[2] YAN, Z., *et al.*, "Pedestal turbulence dynamics in ELMing and ELM-free H-mode plasmas," Fusion Energy 2010 (Proc. 23rd Int. Conf. Daejeon, 2010), IAEA, Vienna (2010), EXC/P3-05.

[3] EVANS, T.E., *et al.*, Nucl. Fusion **48** (2008) 024004.

[4] MORDIJCK, S., *et al.*, Nucl. Fusion **50** (2010) 034006.

[5] GUPTA, D.K., FONCK,R.J., McKEE, G.R., SCHLOSSBERG, D.J., SHAFER, M.W., Rev. Sci. Instrum. **75** (2004) 3493.

[6] HILLESHEIM, J.C., PEEBLES, W.A., RHODES, T.L., SCHMITZ, L., WHITE, A.E., CARTER, T.A., Rev. Sci. Instrum. **81** (2010) 10D907.

[7] SNYDER, P.B., *et al.*, Phys. Plasmas **9** (2002) 2037.

[8] KINSEY, J.E., STAEBLER, G.M., CANDY, J., WALTZ, R.E., BUDNY, R.V., Nucl Fusion **51** (2011) 083001.

[9] SCHMITZ, O., EVANS, T.E, FENSTERMACHER, M.E *et al.*, Nucl. Fusion **52**, 043005 (2012).

[10] BURRELL, K.H., Phys. Plasmas **4** (1997) 1499.

[11] McKEE, G.R., FONCK, R.J., SHAFER, M.W., UZUN-KAYMAK, I.U., YAN, Z., Rev. Sci. Instrum. **81** (2010) 10D741.

[12] SHAFER, M.W, FONCK, R.J., McKEE, G.R. *et al.*, Phys. Plasmas **19**, 032504 (2012).

[13] LECONTE, M.J., and DIAMOND, P., Phys. Plasmas **18** (2011) 082309.

[14] GUPTA, D.K., FONCK, R.J., McKEE, G.R. *et al.,* Phys. Rev. Lett. **97** (2006) 125002.

[15] McKEE, G.R., *et al.*, "Characterization of zonal flows and their dynamics in the DIII-D tokamak, laboratory plasmas, and simulation," Fusion Energy 2006 (Proc. 21st Intl. Conf. Chengdu, 2006), IAEA, Vienna (2006), EX/2-3.

[16] McKEE, G.R., *et al.*, Plasma Phys. Control. Fusion **45** (2003) A477.

[17] SCHAFFER, M.J., *et al.*, Nucl. Fusion **48** (2008) 024004.

ACKNOWLEDGMENT

This work was supported in part by the US Department of Energy under DE-FG02-89ER53296, DE-FG02-08ER54999, DE-FC02-04ER54698, DE-FG02-07ER54917, DE-FG02-05ER54809, DE-AC02-09CH11466 and DE-FG02-08ER54984.